

See discussions, stats, and author profiles for this publication at: <https://www.researchgate.net/publication/231699470>

# Morphology and Phase Transitions in Styrene –Butadiene–Styrene Triblock Copolymer Grafted with Isobutyl–Substituted Polyhedral Oligomeric Silsesquioxanes

ARTICLE *in* MACROMOLECULES · MARCH 2007

Impact Factor: 5.8 · DOI: 10.1021/ma062393d

---

CITATIONS

27

---

READS

23

3 AUTHORS, INCLUDING:



Andre Lee

Michigan State University

71 PUBLICATIONS 1,300 CITATIONS

SEE PROFILE

REPORT DOCUMENTATION PAGE				Form Approved OMB No. 0704-0188	
Public reporting burden for this collection of information is estimated to average 1 hour per response, including the time for reviewing instructions, searching existing data sources, gathering and maintaining the data needed, and completing and reviewing this collection of information. Send comments regarding this burden estimate or any other aspect of this collection of information, including suggestions for reducing this burden to Department of Defense, Washington Headquarters Services, Directorate for Information Operations and Reports (0704-0188), 1215 Jefferson Davis Highway, Suite 1204, Arlington, VA 22202-4302. Respondents should be aware that notwithstanding any other provision of law, no person shall be subject to any penalty for failing to comply with a collection of information if it does not display a currently valid OMB control number. PLEASE DO NOT RETURN YOUR FORM TO THE ABOVE ADDRESS.					
1. REPORT DATE (DD-MM-YYYY) 07-11-2006		2. REPORT TYPE Journal Article		3. DATES COVERED (From - To)	
4. TITLE AND SUBTITLE  Morphology and Phase Transitions in Styrene-Butadiene-Styrene Triblock Copolymer Grafted with Isobutyl Substituted Polyhedral Oligomeric Silsesquioxanes (Postprint)				5a. CONTRACT NUMBER	
				5b. GRANT NUMBER	
				5c. PROGRAM ELEMENT NUMBER	
6. AUTHOR(S) Daniel B. Drazowski & Andre Lee (Michigan State Univ.); Timothy S. Haddad (ERC)				5d. PROJECT NUMBER 23030521	
				5e. TASK NUMBER	
				5f. WORK UNIT NUMBER	
7. PERFORMING ORGANIZATION NAME(S) AND ADDRESS(ES)  Air Force Research Laboratory (AFMC) AFRL/PRSM 9 Antares Road Edwards AFB CA 93524-7401				8. PERFORMING ORGANIZATION REPORT NUMBER  AFRL-PR-ED-JA-2006-439	
9. SPONSORING / MONITORING AGENCY NAME(S) AND ADDRESS(ES)  Air Force Research Laboratory (AFMC) AFRL/PRS 5 Pollux Drive Edwards AFB CA 93524-7048				10. SPONSOR/MONITOR'S ACRONYM(S)	
				11. SPONSOR/MONITOR'S NUMBER(S) AFRL-PR-ED-JA-2006-439	
12. DISTRIBUTION / AVAILABILITY STATEMENT  Approved for public release; distribution unlimited (AFRL-ERS-PAS-2006-281)					
13. SUPPLEMENTARY NOTES © 2007 American Chemical Society. Published in the ACS journal, Macromolecules <b>2007</b> , 40, 2798-2805					
14. ABSTRACT Two symmetric triblock polystyrene-butadiene-polystyrene (SBS) copolymers with different styrene content were grafted with varying amounts of isobutyl-substituted polyhedral oligomeric silsesquioxane (POSS) molecules. The POSS octamers, R'R <sub>7</sub> Si <sub>8</sub> O <sub>12</sub> were designed to contain a single silane functional group, R', which was used to graft onto the dangling 1,2 butadienes in the polybutadiene block and seven identical organic groups, R=isobutyl (iBu). Morphology and phase transitions of these iBu-POSS modified SBS were investigated using small angle X-ray scattering and rheological methods. It was observed that POSS with isobutyl moiety, when grafted to the polybutadiene (PB), appears to show a high affinity to stay within the PB domain; effectively, they enhance the segregation between butadiene and styrene domains. This causes a shift in the phase diagram to lower styrene content. From the rheology, we observed that values of storage modulus, G', at temperatures below the order-disorder transition increase due to the grafting of iBu-POSS. These observations lead us to conclude that the local order morphology between styrene and butadiene domains was better preserved due to the enhanced segregation forced by iBu-POSS.					
15. SUBJECT TERMS					
16. SECURITY CLASSIFICATION OF:			17. LIMITATION OF ABSTRACT  SAR	18. NUMBER OF PAGES  9	19a. NAME OF RESPONSIBLE PERSON Dr. Joseph M. Mabry
a. REPORT Unclassified	b. ABSTRACT Unclassified	c. THIS PAGE Unclassified			19b. TELEPHONE NUMBER (include area code) N/A

# Morphology and Phase Transitions in Styrene–Butadiene–Styrene Triblock Copolymer Grafted with Isobutyl-Substituted Polyhedral Oligomeric Silsesquioxanes

Daniel B. Drazkowski,<sup>†</sup> Andre Lee,<sup>\*,†</sup> and Timothy S. Haddad<sup>‡</sup>

Department of Chemical Engineering & Materials Science, Michigan State University, East Lansing, Michigan 48824, and ERC, Inc., AFRL/PRSM, Edwards AFB, California 93524

Received October 17, 2006; Revised Manuscript Received February 14, 2007

**ABSTRACT:** Two symmetric triblock polystyrene–butadiene–polystyrene (SBS) copolymers with different initial morphologies were grafted with varying amounts of isobutyl-substituted polyhedral oligomeric silsesquioxane (POSS) molecules. The POSS octamers,  $R_7R_8Si_8O_{12}$ , were designed to contain a single silane functional group,  $R'$ , which was used to graft onto the dangling 1,2-butadienes in the polybutadiene block and seven identical organic groups,  $R$  = isobutyl (iBu). Morphology and phase transitions of these iBu-POSS-modified SBS were investigated using small-angle X-ray scattering and rheological methods. It was observed that when iBu-POSS was grafted to the butadiene segment, the long-range and local order of the morphology were preserved, and the  $d$ -spacing showed a small, systematic increase with increasing POSS content. These observations suggest that grafted iBu-POSS were well-distributed within the butadiene domains and did not interact with the styrene domains; effectively, grafting of iBu-POSS to butadiene did not affect the segregation between butadiene and styrene domains. However, addition of iBu-POSS reduces the overall polystyrene volume. Consequently, from a morphology standpoint, this modification effectively shifts the phase diagram to lower styrene content. This was supported with SAXS and transition temperatures measurements made from the different host morphologies.

## Introduction

Block copolymers have been widely used as engineering materials since the early 1960s, and more recently they received interest for uses in nanotechnology. The main focus of their nanotechnology application is rooted in the ability to form self-assembled microstructure on the nanometer scale, which has led to applications in membranes, templates for nanoparticle synthesis, photonic crystals, high-density information storage media, and beyond.<sup>1,2</sup> More recently, block copolymers have been used in conjunction with nanoparticles, and the self-assembled copolymer microstructure has been exploited to control nanoparticle ordering within a particular phase or at the phase interface of the block copolymer matrix.<sup>3,4</sup> Hence, it is critical to gain better understanding on how the surface chemistry of nanoparticles can influence the morphology of block copolymers. To eliminate complications of mixing interactions between particles and others, the problem may be simplified by confining the nanostructures to a particular domain of the block copolymer by grafting nanostructured chemicals to a specific copolymer block.<sup>5,6</sup> We have recently reported that the surface chemistry of the grafted nanostructures has profound effects on the host block copolymer morphology.<sup>5</sup> More specifically, polyhedral oligomeric silsesquioxane (POSS) was used as a model nanostructured chemical and was grafted to the polybutadiene midblock of a symmetric polystyrene-*block*-polybutadiene-*block*-polystyrene copolymer (SBS). Different chemical substituents of POSS (i.e., cyclopentyl (Cp), cyclohexyl (Cy), cyclohexenyl (Cye), and phenyl (Ph)) were studied because of their similar stereochemistry, similar molecular weight, and contrasting electronic properties. It was shown that the morphology of host SBS copolymer became more disrupted

with an increasing amount of grafting, which was supported by a 2-fold increase in primary scattering peak width and the disappearance of high-order scattering peaks. On the basis of these observations and the fact that the POSS were grafted to the butadiene, it was concluded that those POSS investigated favor polystyrene more than polybutadiene. This affinity to the styrene phase leads to a competition between entropic and enthalpic forces: the POSS enthalpically favor the polystyrene phase while disfavoring the polybutadiene phase in which it is grafted, and the POSS entropically favor the polybutadiene phase. This results in a deterioration of the well-segregated interface, which in turn affects the order of the morphology. With the addition of these *interacting* POSS, there is a change from a lamellar to a perforated layer or disrupted morphology as the amount of POSS grafting increases, and the level of perforation and stability of this morphology depends on the degree of POSS–polystyrene compatibility.

These results, although interesting, do not take full advantage of the self-assembled microstructure. The motivation for this work is to create a model system in which nanostructures are confined and dispersed within a single domain of a block copolymer. This model system can be utilized to explore particle–particle and particle–polymer interaction energies, and it can be extended to aid in the design of nanocomposite materials. In order to confine the nanostructures within the grafted domain and maintain a well-segregated morphology, it is necessary to remove the enthalpic interactions which lead to deterioration of the interface. To accomplish this, the surface chemistry of the nanostructure must be selected so it is enthalpically favorable to the domain in which it is grafted and unfavorable to the other block. Isobutyl (iBu) was selected because it has an aliphatic chemistry similar to polybutadiene which contrasts with the aromatic polystyrene. In the following sections, we probe the particle–polymer interaction energies and present results for the morphological changes in SBS grafted

\* To whom correspondence should be addressed: e-mail leea@egr.msu.edu.

<sup>†</sup> Michigan State University.

<sup>‡</sup> ERC, Inc.

Table 1. Comparison of Host SBS<sup>a</sup>

material	$M_w \times 10^{-3}$	$M_n \times 10^{-3}$	PDI	polystyrene content (wt %)	self-assembled morphology	series name
Vector 8508	62	59	1.05	29	cylindrical	C-series
Vector 6241	72	71	1.02	43	lamellar	L-series

<sup>a</sup>  $M_n$  and  $M_w$  (determined by GPC in our laboratory) are number-average and weight-average molecular weights, respectively. PDI is the polydispersity index ( $M_w/M_n$ ). Weight percent of polystyrene is listed by the manufacturer and verified by integration of NMR signals. Self-assembled morphology is determined by small-angle X-ray scattering at room temperature.

with iBu-POSS to the butadiene domain. The iBu-POSS was grafted to SBS in the amounts of 5, 10, and 20 wt %, and two SBS of similar overall degree of polymerization but with different styrene content were used. The morphology of the host SBS was either cylindrical or lamellar depending on the styrene content. Small-angle X-ray scattering (SAXS) was used to quantify the morphological changes in SBS modified by different amounts of grafted iBu-POSS. Additionally, in combination with rheological measurements, we also report morphological transitions and their transition temperatures as a function of POSS content.

## Experimental Section

The host polymers for this study were obtained from Dexcio Polymers: Vector 8508 and Vector 6241. Both are symmetric SBS triblock copolymers and similar in their overall degree of polymerization, but because of their styrene content, they have different morphologies at temperatures far below the order–disorder transition temperature,  $T_{ODT}$ . To avoid continually referencing the abstract material numbers, Vector 8508 will be referred to as the C-series polymer because it has a cylindrical morphology at temperatures far below  $T_{ODT}$ . For similar reasons, Vector 6241 will be referred to as the L-series polymer because it has a lamellar morphology. A more detailed comparison of the two materials is available in Table 1.

POSS grafting was accomplished via a hydrosilation reaction in toluene. The procedures used to synthesize the iBu-POSS hydride and the conditions used for grafting to 1,2-butadiene were identical to our previously reported work.<sup>5</sup> iBu-POSS was grafted to each type of SBS in amounts of 5, 10, and 20 wt %. Samples were prepared in the form of solvent cast films of  $\sim 0.3$  mm thickness. The copolymer samples were dissolved in a toluene, a neutral solvent, in a 3.0 wt % concentration. Approximately 0.1 wt % Irganox 1010 antioxidant (relative to the polymer) was also added to the solution to reduce degradation at high temperatures. The solvent was then allowed to evaporate slowly on glass at 20 °C over a period of 3 days. The films were removed from the glass and were then annealed under vacuum at 60 °C for 7 days.

Small-angle X-ray scattering (SAXS) was used to quantify the morphology changes, since it is capable of examining a large volume of material in the bulk state. The SAXS experiments were performed at beamline 15ID (ChemMatCARS) in the Advanced Photon Source (APS) at Argonne National Laboratory. The energy of radiation used for the experiments was 8.27 keV ( $\Delta E/E \approx 10^{-4}$ ), which corresponds to an X-ray wavelength of 1.50 Å. SAXS patterns were collected using a two-dimensional Bruker 6000 CCD X-ray detector with a  $1024 \times 1024$  pixel array with a  $92 \times 92$   $\mu\text{m}$  pixel size. The camera length was 1.915 m and was calibrated using silver behenate. The SAXS experiments were performed in order to observe the equilibrium morphologies and to verify thermally induced phase transitions. Isothermal experiments were sufficient to observe these phenomena. The protocol implemented for the isothermal experiments included a 10 min annealing time at the required temperature followed by a two-dimensional raster of 1 s exposures covering a  $3 \times 3$  mm area of the film over a 5 min time period. There are several purposes for performing the raster: it minimizes possible beam damage to the sample, it allows for greater statistical sampling, and it ensures that the sample has reached equilibrium.

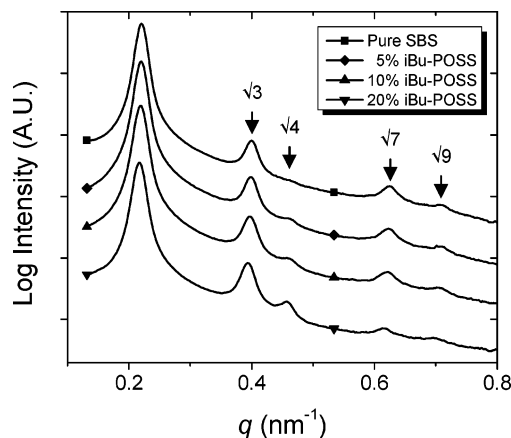


**Figure 1.** Integrated SAXS intensity vs scattering vector,  $q$ , for SBS, Vector 8508, triblock copolymers grafted with isobutyl-POSS at 130 °C. The unmodified Vector 8508 is of cylindrical morphology (C-series). Data are shifted along the log intensity axis to increase clarity.

Small-strain-amplitude oscillatory shear experiments were used to measure the order–order and order–disorder transition temperatures,  $T_{OOT}$  and  $T_{ODT}$ , respectively. Experiments were performed using a TA Instruments AR2000 rheometer with 25 mm parallel plate geometry equipped with an electric heating chamber. Samples were annealed at 150 °C for 5 min and then subjected to a temperature ramp with a heating rate of 2 °C/min. To minimize sample degradation, a dry  $N_2$  purge of 12 mL/min was implemented. The instrument software was used to determine the dynamic storage modulus  $G'(\omega)$  as a function of temperature at a fixed strain amplitude of 2% and oscillatory frequency of 1 rad/s. The onset of each  $G'(\omega)$  vs temperature discontinuity was used to determine the  $T_{OOT}$  and  $T_{ODT}$ . In practice,  $T_{OOT}$  and  $T_{ODT}$  are a function of both frequency and temperature ramp rate, so the listed value does not coincide precisely with the equilibrium transition temperature. However, this calculation is consistently applied throughout the unmodified SBS and POSS–SBS grafted series, and thus the effects of POSS attachments on the transition temperatures are comparable.

## Results and Discussion

We first examine the effects of grafting iBu-POSS to butadiene domains on equilibrium morphology of SBS: the long-ranged and local order and  $d$ -spacing. Comparisons are in the melt state at 130 °C, well below the  $T_{ODT}$ , to ensure equilibrium morphology. We will focus the effects on  $T_{OOT}$  and  $T_{ODT}$  in the Morphology Transitions section which will tie in to theories presented in the Equilibrium Morphology section.

**Equilibrium Morphology.** Figures 1 and 2 show the one-dimensional scattering profiles for all POSS–SBS copolymers investigated as measured by SAXS at 130 °C. Intensity is plotted vs the magnitude of the scattering vector  $q$ .<sup>7</sup> The C-series, which has a cylindrical morphology for the ungrafted SBS, is shown in Figure 1. The scattering patterns of the grafted C-series show little difference from the unmodified SBS. The peak positions are consistent with the structure factor for a hexagonally packed cylindrical morphology ( $1:\sqrt{3}:\sqrt{4}:\sqrt{7}:\sqrt{9}...$ ). Grafting up to 20 wt % iBu-POSS to the host cylindrical morphology has little effect on relative peak position, primary scattering intensity,

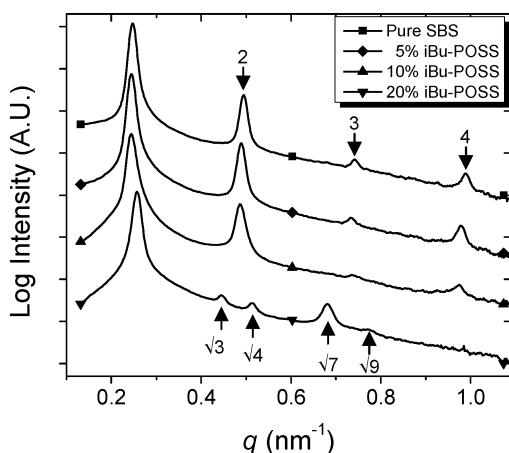


**Figure 2.** Integrated SAXS intensity vs scattering vector,  $q$ , for SBS, Vector 6241, triblock copolymers grafted with isobutyl-POSS at 130 °C. The unmodified Vector 6241 is of lamellar morphology (L-series). Data are shifted along the log intensity axis to increase clarity.

and even the intensities of the high-order  $\sqrt{7}$  and  $\sqrt{9}$  peaks. All of these indicate that the cylindrical morphology is well-preserved after grafting. There is, however, a change in the relative intensity for the third diffraction peak, which will be discussed in more detail later in this section.

Scattering profiles of the L-series, which have varying amounts of iBu-POSS grafted on Vector 6241, are shown in Figure 2. The relative peak positions for the pure, 5%, and 10% are consistent with the structure factor for a lamellar morphology (1:2:3:4...). However, when grafted with 20 wt % iBu-POSS, the observed morphology changes to that of hexagonally packed cylinders. This change in Vector 6241 morphology after grafting can be attributed simply to changes in the overall polystyrene content. By grafting 20 wt % iBu-POSS, the weight fraction of polystyrene is reduced from 43 wt % for the unmodified Vector 6241 to 34 wt % in 20% iBu-POSS grafted Vector 6241. This reduction in polystyrene content is large enough to change the morphology from lamellar to cylindrical. An underlying assumption in this reasoning is that the grafting of iBu-POSS to the polybutadiene does not affect the degree of segregation between the butadiene and styrene domains. Thus, the morphology of modified SBS only depends on the overall volume fraction of a particular block. The argument is in parallel to those studies on highly selective solvent swelling of block copolymers.<sup>8–10</sup> In this case, the iBu-POSS is akin to the solvent molecules that are selective only to the polybutadiene domain. This is a reasonable comparison because the iBu-POSS are chemically grafted to polybutadiene, and thus they are confined within the butadiene domain. As a result, when iBu-POSS is grafted with polybutadiene, the modified POSS–SBS copolymer can be characterized by a resulting shift in composition of the host polymer system along the  $\chi N$  vs  $f$  phase diagram, where  $\chi$  is the Flory–Huggins parameter,  $N$  is the effective degree of polymerization, and  $f$  is the volume fraction of a particular block copolymer component.<sup>9,10</sup>

The hypothesized noninteracting nature of iBu-POSS with the polystyrene domain can be further supported by revisiting the scattering data. The total scattering in Figures 1 and 2 has contributions from interparticle and intraparticle interferences, which are often referred to as lattice and particle scattering, respectively. Lattice scattering determines the structure factor, while the particle scattering exhibits constructive and destructive interference depending on the size and shape of the particle. The diffraction peak disappears when its angular position

**Table 2.** Form Factor Minima for POSS–SBS Copolymers<sup>a</sup>

	wt % POSS	$f_{PS}$ (%)	$q_{m1}/q^*$	$q_{m2}/q^*$
Vector 8508	0	25.6	1.99	3.64
C-series	5	24.6	2.03	3.72
	10	23.5	2.07	3.80
	20	21.3	2.18	3.99
Vector 6241	0	38.9	2.57	5.14
L-series	5	37.3	2.68	5.37
	10	35.6	2.81	5.62
	20	32.2	1.77	3.24

<sup>a</sup> The entire C-series and 20% L-series were calculated using the cylindrical form factor. The lamellar form factor was used for the 0%, 5%, and 10% L-series.  $q_{m1}$  and  $q_{m2}$  are the first and second form factor minima, respectively.  $q^*$  is the position of the primary diffraction peak.

coincides with that of the destructive interference of the particle scattering. Thus, some changes in relative diffraction intensity can be explained by a shift in the scattering form factor minimum, which again is related to the size of the particles contributing to scattering. In the case of the C-series, the polystyrene cylinders, or rods, contribute to the particle scattering. The particle dimension of interest is the cylinder radius.<sup>11,12</sup> Cylinder radius is related to the volume fraction of polystyrene,  $f_{PS}$ , which changes as a result of grafting as stated previously. For the L-series, the thickness of the polystyrene domains contributes to the particle scattering.<sup>11,13–15</sup> The relative thickness of the polystyrene layer thickness to that of the lamellae repeat distance is related to  $f_{PS}$ . The calculations used to derive  $f_{PS}$  and the form factor minima can be found in the Appendix, and the values of the first two form factor minima normalized to the primary scattering peak position are displayed in Table 2 for both the C-series and L-series. The form factor minimum,  $q_m$ , is divided by the primary scattering peak position,  $q^*$ , to obtain  $q_m/q^*$  so it can be related directly to the structure factor.

As mentioned previously for the C-series, there is a change in the relative intensity for the third relative-diffraction peak at position  $\sqrt{4}q^*$ , where  $q^*$  is the position of the primary diffraction peak. This peak is nearly unnoticeable in the unmodified SBS but steadily grows with increased iBu-POSS grafting. For the pure C-series SBS, the first form factor minimum,  $q_{m1}$ , is  $\sim 1.99$  and nearly coincides with the  $\sqrt{4}q^*$  peak. This explains the nearly absent scattering peak. Grafting 5, 10, and 20 wt % POSS reduces the volume fraction. Consequently, the form factor minimum is shifted to higher  $q$ , toward the value of 2.18 for 20 wt % C-series, and away from the  $\sqrt{4}q^*$  peak. The second form factor minimum,  $q_{m2}$ , is outside the range of interest for the C-series in this discussion.

By examining the L-series in Figure 2, one observes a similar shift in the form factor. Here, the  $3q^*$  peak decreases in relative intensity for the 5 wt % and is nearly indistinguishable for the 10 wt %, while the  $4q^*$  peak is still present for both systems. The data in Table 2 show that the first form factor minimum increases from 2.57 for the unmodified SBS to 2.81 for the 10 wt % L-series. The diminishing  $3q^*$  peak corresponds to a shift in form factor minimum toward  $3q^*$ . The 20 wt % L-series has a cylindrical morphology, so its form factor minima calculations show a discontinuity from the rest of the L-series. For this cylindrical morphology, the first minimum in the form factor is at  $1.77q^*$ . This value is between the  $\sqrt{3}q^*$  and  $\sqrt{4}q^*$  peaks and clarifies the relative peak intensity difference when compared to the C-series. The second form factor minimum is at 3.24, near the  $\sqrt{9}q^*$  peak, and can also be related to relative peak intensity differences compared to the C-series. The form factor observations are consistent with iBu-POSS confinement in the polybutadiene domain. This supports the theory that the



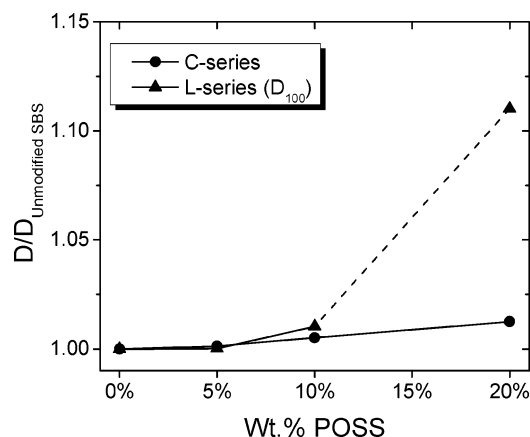


**Figure 3.** The  $d$ -spacing normalized to the unmodified SBS for the C-series and L-series at 130 °C. For the L-series, there is a change in morphology from lamellar (0–10 wt %) to hexagonally packed cylinders (20 wt %).  $D_{100}$  for the cylindrical morphology corresponds to the nearest-neighbor cylinder spacing which is consistent with the lamellar  $d$ -spacing. Error bars are on the order of the symbol size and were removed for clarity. The  $d$ -spacing for unmodified C-series and L-series SBS are 25.71 and 25.41 nm, respectively.

iBu-POSS are confined within the polybutadiene domain and are not interacting with polystyrene.

The lattice spacing, or  $d$ -spacing, values calculated from the primary diffraction peak position<sup>16</sup> for both series of iBu-POSS grafted SBS are shown in Figure 3. For comparison, we normalized measured  $d$ -spacing values of POSS–SBS to the unmodified SBS. For the C-series, a small, but measurable, amount of systematic increase in  $d$ -spacing was observed as the amount of grafted POSS increases. The  $d$ -spacing for block copolymers depends on a number of factors including the degree of polymerization,  $N$ , and monomeric segregation,  $\chi$ . In this system of SBS grafted with POSS, the degree of polymerization does not change, but the overall molecular weight of the macromolecules does. The iBu-POSS is grafted to the polybutadiene block and is subsequently confined there. The iBu-POSS occupies volume within the butadiene phase and may contribute to a greater self-avoiding polymer chain conformation. This results in a more expanded chain conformation for the polybutadiene, which leads to an increase in  $R_g$  for this block. The polystyrene block is unaffected, and the final result is an observed increase in  $d$ -spacing. The monomeric segregation can also affect  $d$ -spacing which may be altered by grafting. The observed increase in  $d$ -spacing shown in Figure 3 along with the preceding  $R_g$  arguments implies that changes in  $\chi$  after grafting iBu-POSS are small. It also confirms that the iBu-POSS does not have favorable compatibility with polystyrene which would reduce  $\chi$  and subsequently the  $d$ -spacing.

For the L-series polymers, the analysis of  $d$ -spacing as affected by grafting iBu-POSS is somewhat more complicated due to the fact that there is a change in the morphology from lamellar to cylindrical morphology as we increase the amount of grafting per chain. The  $d$ -spacing calculated on the basis of the primary peak position of Vector 6241 grafted with 20 wt % iBu-POSS must be multiplied by  $\sqrt{4/3}$  to correspond to the nearest-neighbor distance,  $D_{100}$ , so it can be consistent with the other calculated  $d$ -spacings in the L-series that have a lamellar morphology. As seen in Figure 3, there was an increase of about 10% in the  $d$ -spacing for Vector 6241 grafted with 20 wt % iBu-POSS. This relatively large increase may, in part, be due to the comparison between the cylindrical and lamellar morphologies. However, it is more likely due to the greater volumetric grafting density for the L-series. At the same weight

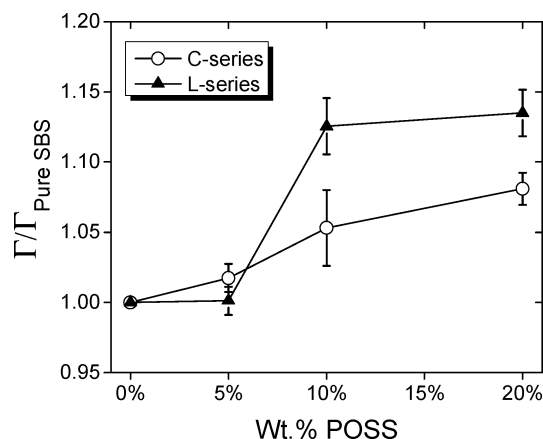


**Figure 4.** Primary scattering peak width,  $\Gamma$ , is normalized to unmodified SBS for the C-series (○) and L-series (▲) at 130 °C. Peak width is measured as the full width at half the maximum peak height. Peak width for unmodified C-series and L-series SBS are 0.0168 and 0.0129 nm<sup>-1</sup>, respectively.

fraction of grafting, both L-series and C-series have nearly equal overall volume fractions of POSS; however, the C-series has more polybutadiene by volume, resulting in a 20% greater volume fraction of POSS within the polybutadiene domain of the corresponding L-series grafting. The consequential confinement of POSS for the L-series may introduce a noticeable POSS–POSS effect that contributes to a larger  $R_g$  for the SBS polymer chain or a greater segregation between the polybutadiene and polystyrene monomers. The increase in  $d$ -spacing observed for the iBu-POSS contrasts to our previous study where the  $d$ -spacing decreases for Vector 6241 grafted with Cy, Cye, and Ph-POSS.

Another quantitative measure of morphology is the full width at one-half of the maximum intensity for the primary peak,  $\Gamma$ . The primary scattering peak width is correlated to the local order of the morphology. Factors that contribute to a broadening of peak width include an increased variance in domain thickness, a limited grain size, defects at grain boundaries, a reduced monomeric segregation at the polystyrene–polybutadiene interface, etc. In Figure 4, the peak width is normalized to unmodified SBS and plotted vs the weight percent of grafted iBu-POSS for both SBS series. Figure 4 shows that the peak width increases with increase in weight percent of POSS grafting. We must note here that the overall peak broadening for both series grafted up to 20 wt % of iBu-POSS is much smaller (on the order of 10%) as compared with the same host SBS block copolymer grafted with Cp, Cy, Cye, and Ph moiety of POSS (on the order of 100%) from the previous study.<sup>5</sup> A large component of the relative increase in peak width is likely due to an introduced polydispersity during the grafting process. Because the POSS attachment is random during the grafting reaction, one can expect a nearly binomial distribution of POSS per chain. This additional variation can also contribute to the small increases in the peak width. In our previous study,<sup>5</sup> a disrupted interface due to a reduced  $\chi$ -parameter contributed to a more substantial peak broadening. The minimal changes in peak width in the present study indicate a well-preserved local morphology of the iBu-POSS–SBS copolymers which gives additional support to the noninteracting nature of iBu-POSS to the styrene domain.

**Morphology Transitions.** The morphology phase behavior as a function of temperature can be examined by the order–disorder and order–order transition temperatures. These transition temperatures were obtained from rheology and determined by abrupt changes in the storage modulus,  $G'$ . For the order–

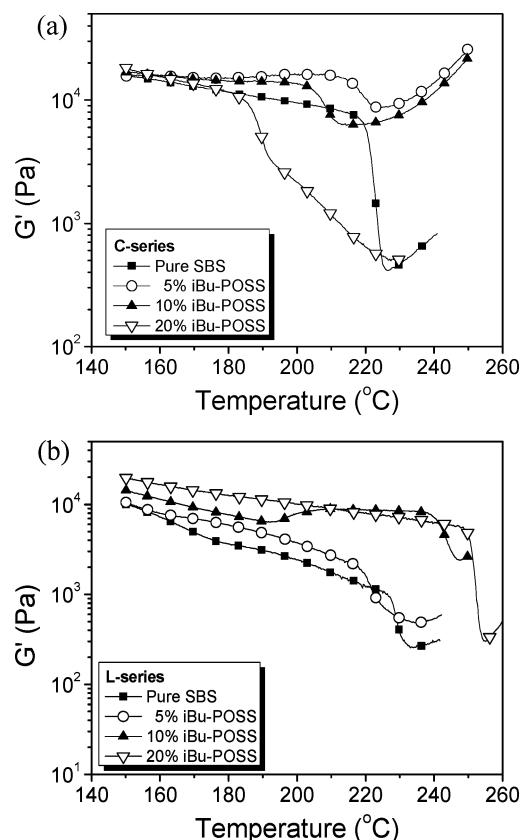


**Figure 5.** Storage modulus,  $G'$ , vs temperature for SBS triblock copolymers grafted with varying amounts of isobutyl-POSS (iBu-POSS) as indicated: (a) the cylindrical host morphology of C-series/Vector 8508 and (b) the lamellar host morphology of L-series/Vector 6241.  $G'$  was obtained using small-strain oscillatory shear with strain amplitude of 2% and oscillatory frequency of 1 rad/s. The temperature ramp rate was 2 °C/min. The rheological experiments were done in a dry nitrogen environment to reduce thermal degradation.

disorder transition temperature,  $T_{ODT}$ , at low frequencies there is a precipitous drop in  $G'$  with increasing temperature, and the onset temperature of this drop is referred to as the  $T_{ODT}$ . The order–order transition temperature,  $T_{OOT}$ , may not always be as evident as the  $T_{ODT}$ . Though there is often a discontinuity in  $G'$ , it may be a discontinuous increase or decrease. Additionally, SAXS measurements were performed near the  $T_{OOT}$  and  $T_{ODT}$  to ensure the accurate designation of transition temperatures and morphologies. Traces of storage modulus,  $G'$ , vs temperature for C-series and L-series of iBu-POSS modified block copolymers are shown in parts a and b of Figure 5, respectively.

In Figure 6, the  $T_{OOT}$  and  $T_{ODT}$  are plotted vs weight percent of iBu-POSS grafted for both series. The entire C-series maintains a cylindrical morphology at all temperatures below  $T_{ODT}$ , and there is a continual decrease in the  $T_{ODT}$  with increased POSS grafting for this series. The L-series phase behavior is more complex. At all temperatures below  $T_{ODT}$ , the unmodified and 5 wt % POSS have a lamellar morphology. Upon heating the L-series 10 wt % iBu-POSS, there is an order–order transition from a lamellar morphology to cylindrical, and upon further heating it undergoes an order–disorder transition. Using SAXS performed at different temperatures as shown in Figure 7, this lamellar to cylindrical transition for the L-series 10 wt % iBu-POSS was clearly observed. The 20 wt % L-series material has a cylindrical morphology at all temperatures below  $T_{ODT}$ .

To put the  $T_{OOT}$  and  $T_{ODT}$  data in the context of the noninteracting/phase shift ideas discussed earlier, the transition

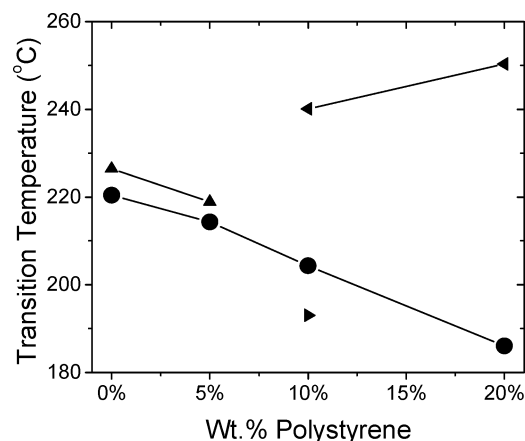


**Figure 6.**  $T_{OOT}$  and  $T_{ODT}$  are plotted for both the C-series and L-series. There is an order–order transition in the L-series for the 10 wt % iBu-POSS. All transitions were verified by SAXS. For the C-series, the ● symbol represents the cylindrical–disorder transition. For the L-series, ▲ represents the lamellar–disorder transition, right-tilted ▲ represents the lamellar–cylindrical transition, and left-tilted ▲ represents the cylindrical–disorder transition.

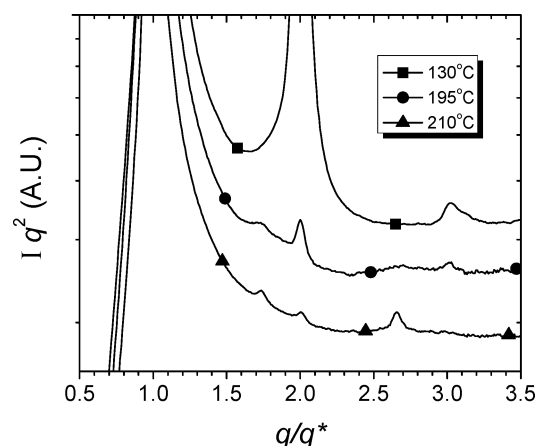


**Figure 7.**  $I q^2$  plotted vs  $q/q^*$  (where  $q^*$  is the  $q$ -position of the primary peak) for L-series 10% iBu-POSS at 130 (■), 195 (●), and 210 °C (▲). The morphology is lamellar morphology at 130 °C. A cylindrical morphology is present near the  $T_{OOT}$ , 195 °C, and at 210 °C the copolymer is well within the cylindrical morphology temperature range.

temperatures are plotted in terms of  $\chi N$  vs  $f_{PS}$  (volume percent of polystyrene) in Figure 8. The solid lines are intended to connect the like transitions of each series, and the dashed lines are extrapolations outside the like transitions to illustrate a relation to the phase shift idea presented earlier in the discussion. The dashed line in the center of the figure relates the C-series and L-series cylindrical morphologies and separates the cylindrical and disordered morphologies. In actuality, we have a ternary system of polystyrene, polybutadiene, and iBu-POSS. However, on the basis of the phase shift arguments mentioned earlier, we plot the data assuming that iBu-POSS grafting only affects the weight fraction of polystyrene and has little effect on segregation between polystyrene and polybutadiene. It is also assumed that  $N$ , the effective degree of polymerization, has not been significantly affected after grafting. The purpose of this plot is not to precisely define the phase space of the POSS–SBS grafts, but to put the  $T_{ODT}$  changes in the context of the reduction of polystyrene content by grafting which was discussed earlier. The values for  $\chi$  were calculated using the fitted parameters obtained by Owens et al.<sup>17</sup>  $N$  was calculated using the average monomer density from the calculations in the Appendix. The transition temperature data are plotted as  $\chi N$  vs  $f_{PS}$  polystyrene show consistency with other styrene–rubber phase dia-

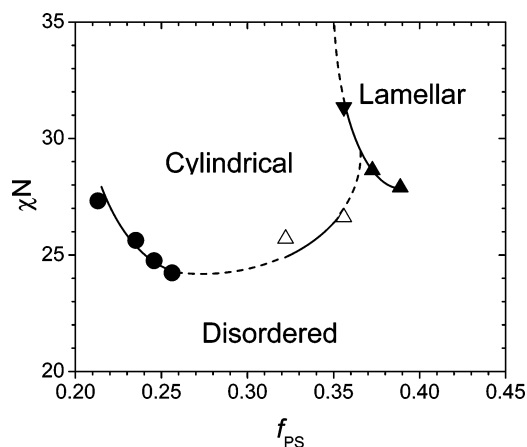


**Figure 8.** Transition temperatures are plotted in terms of  $\chi N$  vs the volume fraction of polystyrene,  $f_{PS}$ , for both SBS series. Unmodified C-series and L-series polymers have 0.256 and 0.389  $f_{PS}$ , respectively. Lines are added to guide the eye and separate the observed morphologies; solid lines connect similar morphology transitions, and dashed lines are extrapolations. For the C-series, the ● symbol represents the cylindrical–disorder transition. For the L-series, ▲ represents the lamellar–disorder transition, ▼ represents the lamellar–cylindrical transition, and △ represents the cylindrical–disorder transition.

grams.<sup>9,10,18–20</sup> Lines are added to guide the eye and separate the observed morphologies. The plot explains the  $T_{ODT}$  drop for the C-series in the context of a shift in composition, it clarifies the  $T_{ODT}$  increase for the 10 and 20 wt % L-series data, and it relates the phase behavior between the two SBS polymer series. It is important to note that no complex phases like the bicontinuous gyroid or the hexagonally perforated lamellae morphologies were observed. It is possible that these phases exist, but they may not have been observable because of their narrow range of stability and the few grafting fractions implemented.

Figure 8 was plotted with three central assumptions: (1) grafting affects the fraction of polystyrene ( $f_{PS}$ ), (2) grafting iBu-POSS does not affect the monomeric segregation between polystyrene and polybutadiene ( $\chi$ ), and (3) the effective degree of polymerization is not affected by grafting ( $N$ ). Support for these has been given in the preceding discussion and all are reasonable within the context of the phase shift argument, but it is important to comment on how deviations from these assumptions will affect Figure 8. The fraction of polystyrene is a straightforward calculation, but it does not take into account the changes due to thermal expansion differences between the polystyrene, polybutadiene, and iBu-POSS. This change is small and will only contribute to a  $f_{PS}$  difference of  $\sim 0.005$  for the 20 wt % iBu-POSS grafts. Grafting does not affect the overall effective degree of polymerization,  $N$ , but it may contribute to a small increase in the chain size,  $R_g$ , as mentioned in the  $d$ -spacing discussion. For grafting fractions of 20 wt % iBu-POSS, this may be a more important factor. The deviation is expected to be only significant for the 20% L-series because it is the only grafted copolymer in this study to deviate more than 2% from the unmodified SBS  $d$ -spacings. If one was to adjust  $N$  for changes in  $R_g$ , it would result in a small vertical shift upward from the uncorrected point on the  $\chi N$  axis. The  $\chi$  parameter also contains a degree of uncertainty.  $\chi$  has been calculated for SB diblocks and triblocks with and without symmetry considerations, but its precise value can vary on the order of a few percent.<sup>17,21,22</sup> The fitted  $\chi$  that was used in Figure 8 was from Owens et al. because the polymer was well-characterized and had similar polydispersity. It is likely that iBu-POSS contributes to changes within the polybutadiene

block, and further studies will be performed. However, it appears that grafting iBu-POSS to the butadiene block of SBS has little effect on the monomeric segregation between the polybutadiene and polystyrene blocks based on what we have seen in the preserved morphology, small increases in  $d$ -spacing and peak width, and the  $T_{OOT}$  and  $T_{ODT}$  behavior.

## Conclusions

In this work, we investigated the phase behavior and morphology changes of SBS grafted with iBu-POSS. Two host SBS morphologies were examined at 0, 5, 10, and 20 wt % grafting. The morphology and phase behavior observed for both systems are consistent with that of a shift in polystyrene content with little change in  $\chi$ . This supports the theory that iBu-POSS is confined within the polybutadiene domain and is noninteracting with polystyrene. The local and long-ranged order of the morphology is preserved for all SBS grafted with iBu-POSS copolymers investigated. There is a small, systematic change in the  $d$ -spacing for both the cylindrical and lamellar morphologies. The 20 wt % L-series has the largest  $d$ -spacing change and may result from comparing cylindrical to lamellar morphologies or from the higher polybutadiene volumetric grafting density compared to the other SBS grafted with iBu-POSS copolymers. The selective swelling/phase shift behavior is again illustrated in the order–order and order–disorder morphology transitions. The transition temperatures are highly correlated to the polystyrene content, and the phase behavior is comparable to other styrene–rubber phase diagrams. Using the prescribed system of grafting nanostructures of precise chemistry to a well-characterized host copolymer, this study offers a way of incorporating nanostructures to block copolymers while having precise control of the resulting morphology, domain sizes, and transition temperatures.

**Acknowledgment.** This research was partially supported by the Air Force Research Laboratory at Edwards AFB, CA, and the Air Force Office of Scientific Research. We are also thankful to ChemMatCARS for the use of their small-angle X-ray scattering facility at the Advanced Photon Source, Argonne National Laboratory. ChemMatCARS is principally supported by the National Science Foundation/Department of Energy under Grant CHE0087817. The Advanced Photon Source is supported by the U.S. Department of Energy, Basic Energy Sciences, Office of Science, under Contract W-31-109-Eng-38.

## Appendix

**Calculation for Volume Fraction of Polystyrene.** The volume percent polystyrene,  $f_{PS}$ , was calculated using bulk densities of 1.05 and 0.887 g/cm<sup>3</sup> for polystyrene and polybutadiene, respectively. The density of the iBu-POSS hydride was estimated to be 1.15 g/cm<sup>3</sup> based on measurements of Larsson.<sup>23,24</sup>

$$f_{PS} = \frac{\rho_g}{\rho_{PS}} W_{PS}$$

$$\rho_g = \frac{1}{W_{PS}/\rho_{PS} + W_{PB}/\rho_{PB} + W_{POSS}/\rho_{POSS}}$$

where  $\rho_{PS}$ ,  $\rho_{PB}$ ,  $\rho_{POSS}$ , and  $\rho_g$  are the densities for polystyrene,



$$\rho_g = \frac{1}{(1 - W_{\text{POSS}})(W_{\text{PSO}}/\rho_{\text{PS}} + (1 - W_{\text{PSO}})/\rho_{\text{PB}}) + W_{\text{POSS}}/\rho_{\text{POSS}}}$$

$$V_{\text{PS}} = \frac{W_{\text{PSO}}(1 - W_{\text{POSS}})/\rho_{\text{PS}}}{(1 - W_{\text{POSS}})(W_{\text{PSO}}/\rho_{\text{PS}} + (1 - W_{\text{PSO}})/\rho_{\text{PB}}) + W_{\text{POSS}}/\rho_{\text{POSS}}}$$

polybutadiene, iBu-POSS hydride, and the POSS-SBS grafted system, respectively.  $W_{\text{PS}}$ ,  $W_{\text{PB}}$ , and  $W_{\text{POSS}}$  are the weight fractions for polystyrene, polybutadiene, and iBu-POSS hydride for a particular POSS-SBS grafted system. The expression can be made more general by using the densities and the polystyrene weight fraction of the original SBS,  $W_{\text{PSO}}$ , and the weight fraction of POSS grafted,  $W_{\text{POSS}}$ . It is important to note that the above calculations assume no change in volume upon mixing and do not take into account differences in thermal expansion. Calculated  $f_{\text{PS}}$  for the C-series and L-series copolymers can be found in Table 2.

**Calculations for Form Factor Minima.** The cylindrical morphology of the C-series SBS is modeled as an arrangement of polystyrene cylinders aligned in a hexagonally packed manner. The hexagonal packing (interparticle order) yields the typical structure factor for the cylindrical morphology (1,  $\sqrt{3}$ ,  $\sqrt{4}$ ,  $\sqrt{7}$ ,  $\sqrt{9}$ , ...). The polystyrene cylinders themselves also contribute to the scattering profile through particle scattering or the form factor. The structure amplitude for a cylindrical or rodlike particle,  $F(q)$ , where the length of the rod is much larger than the radius and in scattering directions orthogonal to the cylindrical axis scales by the relation:<sup>11,12</sup>

$$F(q) \sim \frac{J_1(qR)}{qR}$$

where  $J_1$  is the Bessel function of the first kind of order 1,  $q$  is the magnitude of the scattering vector, and  $R$  is the cylinder radius. In block copolymers, the cylinders have an interfacial thickness which contributes to an additional damping factor which does not contribute to the position of the scattering minima. Observed scattering intensity, scales as  $F^2(q)$ . The minimum intensity in this form factor can be found when  $J_1(qR) = 0$  for values of  $q > 0$ . If we denote  $S_i$  as a solution to the equation  $J_1(x) = 0$ , then the  $q$  at which the form factor is at a minimum (denoted here as  $q_m$ ) is related to the cylinder radius by

$$q_m = \frac{S_i}{R}$$

The volume fraction of polystyrene,  $f_{\text{PS}}$ , can be related to the cylinder radius, nearest-neighbor cylinder distance ( $a = D_{100}$ ), and the  $d$ -spacing of the primary scattering peak,  $d_*$ .

$$f_{\text{PS}} = \frac{2\pi R^2}{\sqrt{3} a^2}, \quad d_* = \frac{\sqrt{3}}{2} a$$

$$f_{\text{PS}} = \frac{\sqrt{3}\pi R^2}{2 d_*^2}, \quad R = \sqrt{\frac{2d_*^2 f_{\text{PS}}}{\sqrt{3}\pi}}$$

The form factor minimum,  $q_m$ , is most easily compared to the morphology structure factor by the dimensionless ratio  $q_m/q^*$ .

$$q_m = S_i \sqrt{\frac{\sqrt{3}\pi}{2d_*^2 f_{\text{PS}}}}; \quad \frac{q_m}{q^*} = S_i \sqrt{\frac{\sqrt{3}}{8\pi f_{\text{PS}}}}$$

The solutions,  $S_i$ , to  $J_1(x) = 0$  are approximately 3.83171, 7.01559, 10.1735, .... Values for the first two solutions of  $q_m/q^*$  can be found in Table 2.

In the case of the L-series, the structure amplitude for lamellae, or flat particles, whose in-plane dimensions are much greater than the thickness and spacing dimensions scales by<sup>11,14</sup>

$$F(q) \sim \frac{\sin(qT/2)}{qT/2}$$

where  $q$  is the magnitude of the scattering vector and  $T$  is the thickness of the lamellae. Observed scattering intensity scales as  $F^2(q)$ . The minimum in this form factor can be found when  $\sin(qT/2) = 0$  for values of  $q > 0$ . The solution to this equation takes the form  $qT/2 = \pi n$ , where  $n$  is a positive integer (for  $q > 0$ ). The relationships of  $q_m$  and  $q_m/q^*$  to  $f_{\text{PS}}$  are

$$q_m = \frac{2\pi}{T} n = \frac{2\pi}{f_{\text{PS}} D} n; \quad \frac{q_m}{q^*} = \frac{1}{f_{\text{PS}}} n$$

Values for the first two solutions of  $q_m/q^*$  can be found in Table 2.

The calculations relating  $f_{\text{PS}}$  to the polystyrene cylinder radius and lamellae thickness assume that the entire volume of iBu-POSS is confined within the polybutadiene domain. In practice, the polystyrene cylinders and lamellae possess a size distribution, interfacial curvature, and interfacial thickness rather than existing as monodisperse hard particles. In addition, the orientation of the particles (cylinders and lamellae) is random in the plane of the film. Consequently, the form factor minima will not result in complete destructive interference, but it will result in reduced structure factor intensity.

**Calculation for  $N$ .** The parameters and notation used in the calculation of  $N$  are the same as those used by Owens et al.<sup>17</sup>  $N$  was normalized to constant monomer volume according to the geometric average by the following relations:

$$\rho^* = \left( \prod_{i=1}^n \rho_i \right)^{1/n}$$

$$b_i^* = b_i \sqrt{\rho_i / \rho^*} \rho \lambda \xi$$

$$N_i^* = N_i (b_i / b_i^*)^2$$

where  $\rho_i$  is the monomeric density of the  $i$ th component,  $\rho^*$  is the average monomer density,  $b$  is the statistical segment length, and  $N$  is the degree of polymerization. The monomeric density for polystyrene and polybutadiene used in the calculations are based on bulk densities of 1.05 and 0.887 g/cm<sup>3</sup>, respectively (to achieve 10 100 and 16 400 mol/m<sup>3</sup>, respectively).

## References and Notes

- (1) Park, C.; Yoon, J.; Thomas, E. L. *Polymer* **2003**, *44*, 6725.
- (2) Förster, S.; Antonietti, M. *Adv. Mater.* **1998**, *10*, 1995.
- (3) Fink, Y.; Urbas, A. M.; Bawendi, M. G.; Joannopoulos, J. D.; Thomas, E. L. *J. Lightwave Technol.* **1999**, *17*, 1963.
- (4) Fogg, D. E.; Radzilowski, L. H.; Blanski, R.; Schrock, R. R.; Thomas, E. L. *Macromolecules* **1997**, *30*, 417.
- (5) Drazkowski, D. B.; Lee, A.; Haddad, T. S.; Cookson, D. J. *Macromolecules* **2006**, *39*, 1854.
- (6) Fu, B. X.; Lee, A.; Haddad, T. S. *Macromolecules* **2004**, *37*, 5211.

- (7)  $q = 4\pi(\sin \theta)/\lambda$  where  $2\theta$  is the scattering angle and  $\lambda$  is the wavelength of radiation.
- (8) Lai, C.; Russel, W. B.; Register, R. A. *Macromolecules* **2002**, *35*, 841.
- (9) Hanley, K. J.; Lodge, T. P.; Huang, C. I. *Macromolecules* **2000**, *33*, 5918.
- (10) Lodge, T. P.; Pudil, B.; Hanley, K. J. *Macromolecules* **2002**, *35*, 4707.
- (11) Glatter, O.; Kratky, O. *Small Angle X-ray Scattering*; Academic Press: New York, 1982.
- (12) Hashimoto, T.; Kawamura, T.; Harada, M.; Tanaka, H. *Macromolecules* **1994**, *27*, 3063.
- (13) Sakurai, S.; Okamoto, S.; Kawamura, T.; Hashimoto, T. *J. Appl. Crystallogr.* **1991**, *24*, 679.
- (14) Shibayama, M.; Hashimoto, T. *Macromolecules* **1986**, *19*, 740.
- (15) Koizumi, S.; Hasegawa, H.; Hashimoto, T. *Macromolecules* **1994**, *27*, 7893.
- (16)  $d = 2\pi/q^*$ , where  $d$  is the  $d$ -spacing (repeat distance) and  $q^*$  is the primary peak position.
- (17) Owens, J. N.; Gancarz, I. S.; Kobertstein, J. T.; Russell, T. P. *Macromolecules* **1989**, *22*, 3380.
- (18) Förster, S.; Khandpur, A. K.; Zhao, J.; Bates, F. S.; Hamley, I. W.; Ryan, A. J.; Bras, W. *Macromolecules* **1994**, *27*, 6922.
- (19) Khandpur, A. K.; Förster, S.; Bates, F. S.; Hamley, I. W.; Ryan, A. J.; Bras, W.; Almdal, K.; Mortensen, K. *Macromolecules* **1995**, *28*, 8796.
- (20) Lodge, T. P.; Hanley, K. J.; Pudil, B.; Alapperuma, B. *Macromolecules* **2003**, *36*, 816.
- (21) Hewel, M.; Ruland, W. *Makromol. Chem., Macromol. Symp.* **1986**, *4*, 1997.
- (22) Sakurai, S.; Mori, K.; Okawara, A.; Kimishima, K.; Hashimoto, T. *Macromolecules* **1992**, *25*, 2679.
- (23) Larsson, K. *Ark. Kemi* **1960**, *16*, 209.
- (24) Kopesky, E. T.; Haddad, T. S.; Cohen, R. E.; McKinley, G. H. *Macromolecules* **2004**, *37*, 8992.

MA062393D